

Rate Constant and Product Branching for the Vinyl Radical Self Reaction at $T = 298$ K

R. P. Thorn,[†] W. A. Payne,[‡] and L. J. Stief*

Laboratory for Extraterrestrial Physics, Code 691, NASA/Goddard Space Flight Center, Greenbelt, Maryland 20771

D. C. Tardy*

Department of Chemistry, University of Iowa, Iowa City, Iowa 52242

Received: March 16, 1996; In Final Form: May 17, 1996[⊗]

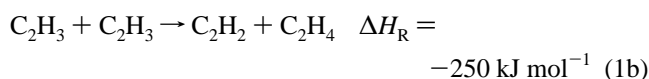
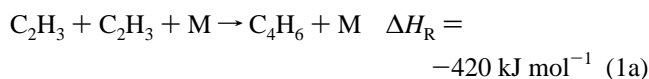
The rate constant and product branching for the self reaction of C_2H_3 has been measured using the discharge–flow kinetic technique coupled to mass spectrometric detection at $T = 298$ K and 1 Torr nominal pressure (He). C_2H_3 is produced by the reaction of F with C_2H_4 , which also forms $C_2H_3F + H$. In addition to the C_2H_3 self reaction, C_2H_3 also decays by reaction with H and by wall loss processes. The result obtained by parameter fitting the C_2H_3 decay curves was $k(C_2H_3 + C_2H_3) = (1.41 \pm 0.60) \times 10^{-10} \text{ cm}^3 \text{ molecule}^{-1} \text{ s}^{-1}$, where k is defined by $d[C_2H_3]/dt = 2k[C_2H_3]^2$. Results from the product studies showed that the recombination product 1,3-butadiene was not observed at 1 Torr and that the ratio $[C_2H_2]$ product formed/ $[C_2H_3]_0$ was 0.65 ± 0.14 for the combined $C_2H_3 + C_2H_3$ and $C_2H_3 + H$ reactions. Both observations are consistent with $C_2H_2 + C_2H_4$ being the exclusive $C_2H_3 + C_2H_3$ products, since the maximum yield of C_2H_2 from the combined $C_2H_3 + C_2H_3$ and $C_2H_3 + H$ reactions is 0.59. The experimental observations that k_1 is independent of pressure and that no 1,3-butadiene (product of C_2H_3 combination) is observed at 1 Torr pressure requires a mechanism in which the chemically activated 1,3-butadiene undergoes a unimolecular reaction. It is postulated that the 1,3-butadiene first isomerizes to cyclobutene, which then unimolecularly decomposes to C_2H_2 and C_2H_4 . Although the former reaction is well documented, the latter reaction has not been previously reported. RRKM calculations predict a pressure dependence similar to what is experimentally observed.

Introduction

Vinyl radical reactions at low temperatures have importance in the hydrocarbon photochemistry that occurs in atmospheres of the outer planets^{1,2} and satellites^{3,4} as well as in dense interstellar clouds.⁵ Reactions of the vinyl radical are significant in such systems, since they can serve both to interconvert C_2 hydrocarbon species and to generate the higher-order organics (C_3 , C_4 , etc.) that eventually form stratospheric hazes.¹ At high temperatures, vinyl radical reactions occur in hydrocarbon pyrolysis and combustion processes.⁶ The reaction kinetics data base of the vinyl radical is limited owing to difficulties in cleanly generating and monitoring C_2H_3 . Vinyl reaction rate constants have been estimated using *ab initio*,⁷ RRK(M),⁸ and other theoretical methods.⁹ At $T = 298$ K, absolute or relative rate constants have been determined for the reactions of vinyl with Cl_2 ,¹⁰ O_2 ,^{11–13a} CH_3 ,¹⁴ O ,¹⁵ HCl ,¹³ C_2H_5 ,¹⁶ N ,¹⁷ HCN ,¹⁸ H ,^{14,15,19,20} and H_2 .²¹

The C_2H_3 self reaction has the potential to be important in both the relatively low temperatures of planetary atmospheres and the elevated temperatures of combustion processes. Furthermore, the vinyl self reaction is a likely side reaction in laboratory studies of the C_2H_3 photochemical system and a more definitive knowledge of the rate constant and the product branching ratios would assist interpretation of experiments designed to study other vinyl reactions important in atmospheric and combustion chemistry. There have been three direct measurements^{14,22,23} of the rate constant for the C_2H_3 self reaction at 298 K reported in the literature and one recent

measurement at 623 K.²⁴ However, the reported 298 K rate constant values differ by more than a factor of 20. Also, there have been numerous measurements^{25–30} reported on the combination/disproportionation ratio of vinyl radicals in the gas phase.



There is an even larger uncertainty in the ratio k_{1a}/k_{1b} with reported values varying from 1 to 50.^{26–30} The majority of the earlier studies did not have a clean and well-defined radical source, and this resulted in secondary chemistry affecting the kinetic analysis.

All of the three previous flash photolysis studies^{14,22,23} had uncertainties in the initial radical concentration owing to uncertainties in the vinyl quantum yield from the photolytic precursor divinyl ether²³ ($C_2H_3OC_2H_3$) or divinyl mercury^{14,22} ($C_2H_3HgC_2H_3$). MacFadden and Currie²³ monitored the decay of C_2H_3 via time-of-flight mass spectrometry and determined the initial C_2H_3 concentration from the measured decrease in $C_2H_3OC_2H_3$ concentration, assuming unit quantum yield for C_2H_3 formation. This early first direct study of reaction 1 was performed at low pressures (65–200 mTorr). Fahr and Laufer²² used vacuum-UV flash photolysis kinetic absorption spectroscopy to monitor the decay of the reactant radical C_2H_3 . In a later study by Fahr *et al.*¹⁴ a rate constant value was obtained by observing the temporal buildup of the product molecule C_4H_6 (1,3-butadiene) using UV laser photolysis kinetic absorption spectroscopy. In both cases, gas chromatographic analysis of

* To whom correspondence should be addressed. E-mail: u1ljs@lepvax.nasa.gov. E-mail: dwight-tardy@uiowa.edu.

[†] NAS/NRC Research Associate. E-mail: ysprt@lepvax.gsfc.nasa.gov.

[‡] E-mail: u1wap@lepvax.gsfc.nasa.gov.

[⊗] Abstract published in *Advance ACS Abstracts*, July 1, 1996.

final products was used to better estimate the initial C₂H₃ concentration. In the latest study by Fahr *et al.*²⁵ methyl vinyl ketone was the photolytic source used to determine the combination/disproportionation ratio for the vinyl self reaction. The recent flash photolysis studies^{14,22} were performed at high pressure (100 and 400 Torr He).

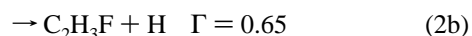
In this present work we have determined k_1 and the product branching ratios at low pressure and $T = 298$ K. The measurements were undertaken using the discharge–flow kinetic technique coupled to mass spectrometric detection of the vinyl radical at a nominal pressure of 1 Torr (He). Initial radical concentrations were determined by direct titration. A RRKM unimolecular decomposition calculation is applied to the excited C₄H₆ adduct in order to determine mechanistic pathways.

Experimental Section

Discharge Flow Reactor. All experiments were performed in a Pyrex flow tube, ~60 cm long and 28 mm in diameter, the inner surface of the tube being lined with Teflon. The flow tube was used at ambient temperatures. The flow tube was coupled *via* a two-stage stainless steel collision-free sampling system to a quadrupole mass spectrometer (Extrel, Inc.) that was operated at low electron energies (typically <20 eV) in order to minimize fragmentation. For example, a nominal ionization energy of 11.5 eV was employed to monitor the C₂H₃ radical, thereby minimizing formation of C₂H₃⁺ *via* dissociative ionization of C₂H₄.³¹ The expected stable end products C₂H₂ and C₄H₆ were also monitored at ~11.5 eV. Ions were detected by an off axis channeltron multiplier (Galileo Electro Optics Corp.). Molecular reactants were admitted *via* a Pyrex movable injector, the position of which could be changed between 2 and 40 cm from the sampling point. This system has been described in detail previously.^{32,33}

Helium carrier gas was flowed at 725 cm³ min⁻¹ (STP) into the reaction vessel. The linear flow velocity ranged from 2460 to 2530 cm s⁻¹ at nominal pressures in the region of 1 Torr (133.32 Pa). In the calculation of the linear flow velocity, the plug flow assumption was made. The flow velocity is calculated from the gas constant, temperature, cross-sectional area of the flow tube, total gas flow, and total pressure. Gas flows were measured and controlled by electronic flow meters (MKS). A side arm, at the upstream end of the flow tube, contained a microwave discharge (<70W, 2450 MHz) for the production of atomic species.

Production of C₂H₃. Fluorine atoms were produced at the upstream end of the flow reactor by passing molecular F₂ (*ca.* 5% diluted in helium) or CF₄ (*ca.* 1% diluted in helium) through a microwave discharge; up to 70% of the F₂ and 37% of the CF₄ were dissociated in the discharge. The discharge region consisted of a 3/8 in. ceramic tube mounted inside the discharge arm. When CF₄ was used, a recombination volume³⁴ was placed downstream from the microwave discharge to allow CF_x to recombine.³⁵ The volume was 10 cm in length, 7 cm diameter Pyrex glass, giving a residence time of *ca.* 60 ms. At the tip of the sliding injector C₂H₃ was produced *via* the reaction



$$k_2(T=298 \text{ K}) = 2.7 \times 10^{-10} \text{ cm}^3 \text{ molecule}^{-1} \text{ s}^{-1} \text{ (ref 36)}$$

the branching ratio (Γ) having been determined by Slagle and Gutman.³⁷ Formation of C₂H₃ was essentially complete within 2–3 cm of the injector tip.

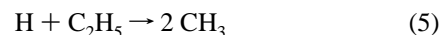
Titration of F. Absolute F atom concentrations were determined by the fast titration reaction



$$k_3(T=298 \text{ K}) = 1.6 \times 10^{-10} \text{ cm}^3 \text{ molecule}^{-1} \text{ s}^{-1} \text{ (ref 38)}$$

The F atom concentration was determined by measuring the decrease in the Cl₂⁺ signal ($m/z = 70$) when the discharge was initiated. The absolute F concentration is given by $[\text{F}] = [\text{Cl}_2]_{\text{disch off}} - [\text{Cl}_2]_{\text{disch on}}$. As discussed previously for N atom studies,³⁹ a number of precautions were taken in order to avoid systematic errors in this type of measurement. Resultant [C₂H₃]₀ was calculated as 0.35[F]₀. Vinyl radical concentrations were in the region of (0.4–2.9) × 10¹² molecule cm⁻³ for the k_1 rate determination decays and (0.9–2.9) × 10¹¹ molecule cm⁻³ for the first-order loss decays.

Production of CH₃. Recent experiments have shown that methyl radical, CH₃, is concurrently present in the flow tube during the production and decay of C₂H₃. The CH₃ is generated on a considerably longer time scale than the C₂H₃ as the CH₃ signal continues to rise at $t > 10$ ms. Some CH₃ generation can be expected to occur through the two reaction sequences:



$$k_4(T=298 \text{ K}) = 6.8 \times 10^{-14} \text{ cm}^3 \text{ molecule}^{-1} \text{ s}^{-1} \text{ at 1 Torr He pressure (ref 40)}$$

$$k_5(T=298 \text{ K}) = 6.0 \times 10^{-11} \text{ cm}^3 \text{ molecule}^{-1} \text{ s}^{-1} \text{ (ref 6)}$$

Experiments consisted of monitoring the net CH₃ signal ($m/z = 15$) at 11.5 eV as a function of time with both the F₂ source on and C₂H₄ flowing through the injector. No CH₃ was observed in the absence of C₂H₄ (with the F atom source on) or in the absence of F (with C₂H₄ present). The well-known F + CH₄ reaction was used to obtain the CH₃ signal calibration under conditions where [CH₃]₀ is equal to [F]₀. For these CH₃ generation experiments, absolute concentrations of F atoms were determined by the fast titration reaction with CH₄.⁴¹

To investigate the net CH₃ signal specifically resulting from reactions 4 and 5, an experiment using an H atom source was performed. The well-known F + H₂ reaction⁴² was used to generate H at the rear of the flow tube, and C₂H₄ was added *via* the movable injector. The initial H present was determined by titration with NO₂.⁴¹ The [CH₃] temporal profile obtained was similar to the [CH₃] profiles obtained without H₂ present (*i.e.*, in the production of C₂H₃ and H *via* F + C₂H₄) but was ~50% lower in net signal for the same [H]₀. The CH₃ temporal profile showed an abrupt initial [CH₃] rise ($t < 1.5$ ms) and then a slow rise on a time scale typical of production from reactions 4 and 5.

Further experiments were performed to determine if the CH₃ present was dependent upon the presence of C₂H₃. An experiment performed with excess O₂ present ([O₂]₀/[C₂H₃]₀ = 84) to scavenge C₂H₃ showed a CH₃ net signal temporal profile similar to those obtained without O₂. It is doubtful that the presence of CH₃ is associated with a C₂H₃ reaction or a product of a C₂H₃ reaction. Furthermore, because the time scale for CH₃ generation is much longer than that for C₂H₃ generation, it is very unlikely that the CH₃ generated results from a mechanism that consumes F on this same time scale.

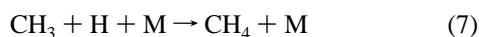
TABLE 1: Chemical System and Rate Constants Used in the Numerical Models

no.	reaction	$k(298\text{ K})^a$	ref
Primary Reactions			
1a	$\text{C}_2\text{H}_3 + \text{C}_2\text{H}_3 + \text{M} \rightarrow \text{C}_4\text{H}_6 + \text{M}$	$\leq 10^{-12\text{ c,d}}$	this study
1b	$\text{C}_2\text{H}_3 + \text{C}_2\text{H}_3 \rightarrow \text{C}_2\text{H}_4 + \text{C}_2\text{H}_2$	1.4×10^{-10}	this study
2a	$\text{F} + \text{C}_2\text{H}_4 \rightarrow \text{C}_2\text{H}_3 + \text{HF}$	9.4×10^{-11}	36
2b	$\text{F} + \text{C}_2\text{H}_4 \rightarrow \text{C}_2\text{H}_3\text{F} + \text{H}$	1.8×10^{-10}	36
10a	$\text{C}_2\text{H}_3 + \text{H} + \text{M} \rightarrow \text{C}_2\text{H}_4 + \text{M}$	$3.6 \times 10^{-11\text{ c}}$	19
10b	$\text{C}_2\text{H}_3 + \text{H} \rightarrow \text{C}_2\text{H}_2 + \text{H}_2$	7.4×10^{-11}	19
12	$\text{C}_2\text{H}_3 \rightarrow \text{first-order decay}$	see Table 2	this study
Secondary Reactions			
4	$\text{H} + \text{C}_2\text{H}_4 + \text{M} \rightarrow \text{C}_2\text{H}_5 + \text{M}$	$6.8 \times 10^{-14\text{ c}}$	40
11a	$\text{C}_2\text{H}_3 + \text{CH}_3 \rightarrow \text{C}_3\text{H}_6$	1.1×10^{-10}	14, 25
11b	$\text{C}_2\text{H}_3 + \text{CH}_3 \rightarrow \text{C}_2\text{H}_2 + \text{H}_2$	3.6×10^{-11}	14, 25
6	$\text{CH}_3 + \text{CH}_3 + \text{M} \rightarrow \text{C}_2\text{H}_6 + \text{M}$	$6.0 \times 10^{-11\text{ c}}$	44
7	$\text{CH}_3 + \text{H} + \text{M} \rightarrow \text{CH}_4 + \text{M}$	$2.0 \times 10^{-12\text{ c}}$	45
8	$\text{CH}_3 \rightarrow \text{first-order decay}$	3^b	this study
9	$\text{H} \rightarrow \text{first-order decay}$	20^b	46
	0-order source $\rightarrow \text{CH}_3$	$38.1 \times [\text{F}]_0^e$	this study
15	$\text{H} + \text{F}_2 \rightarrow \text{HF} + \text{F}$	2.5×10^{-12}	47
16	$\text{CH}_3 + \text{F}_2 \rightarrow \text{CH}_3\text{F} + \text{F}$	1.0×10^{-12}	48

^a Rate constant units are in $\text{cm}^3 \text{ molecule}^{-1} \text{ s}^{-1}$ except where noted.

^b Units in s^{-1} . ^c Values at $P = 1$ Torr He. ^d Upper limit for k_{1a} . A value of zero was used for modeling purposes. ^e Source rate in units of $\text{molecule cm}^{-3} \text{ s}^{-1}$.

Three separate experiments were performed to characterize the CH_3 generation process at a range of conditions similar to those of the vinyl decay experiments: $3.0 \times 10^{12} < [\text{F}]_0 < 8.5 \times 10^{11} \text{ molecule cm}^{-3}$; $[\text{C}_2\text{H}_4]_0 = 1.3 \times 10^{14} \text{ molecule cm}^{-3}$; $T = 298 \text{ K}$ and $P = 1$ Torr He. The net CH_3 signal was observed to rise at a decreasing rate until it leveled off at $t > 16 \text{ ms}$. This asymptotic CH_3 signal level was proportional to $[\text{F}]_0$. Most importantly, at $t = 16 \text{ ms}$, the $[\text{CH}_3]$ level was observed to equal 20–25% of $[\text{F}]_0$, which is a 20-fold excess over the $[\text{CH}_3]$ level predicted by numerical modeling (FACSIMILE program⁴³) using the reaction sequence 4 and 5 as the sole CH_3 source but is within a factor of 2 of that observed in the $\text{H} + \text{C}_2\text{H}_4$ experiments designed to measure the effect of the reaction sequence 4 and 5. In addition to reactions 4 and 5, the reaction scheme (Table 1) included C_2H_3 generation and loss reactions, H generation and loss reactions, and the following CH_3 loss reactions:



$\text{CH}_3 \rightarrow \text{decay by first-order processes}$
including wall reactions (8)

$\text{H} \rightarrow \text{decay by first-order processes}$
including wall reactions (9)

$$k_6(T=298 \text{ K}, P=1 \text{ Torr He}) = 6.0 \times 10^{-11} \text{ cm}^3 \text{ molecule}^{-1} \text{ s}^{-1} \text{ (ref 44)}$$

$$k_7(T=298 \text{ K}, P=1 \text{ Torr He}) = 2.0 \times 10^{-12} \text{ cm}^3 \text{ molecule}^{-1} \text{ s}^{-1} \text{ (ref 45)}$$

$$k_9(T=298 \text{ K}, P=1 \text{ Torr He}) = 20 \text{ s}^{-1} \text{ (ref 46)}$$

A series of independent experiments based on the fast $\text{F} + \text{CH}_4$ reaction as a CH_3 source determined $k_8(T=298 \text{ K}, P=1 \text{ Torr He}) = 3 \text{ s}^{-1}$.

The $[\text{CH}_3]$ temporal profiles were simulated to an excellent degree by including a generic zeroth-order CH_3 generation mechanism instead of reaction 5. The CH_3 source rate was

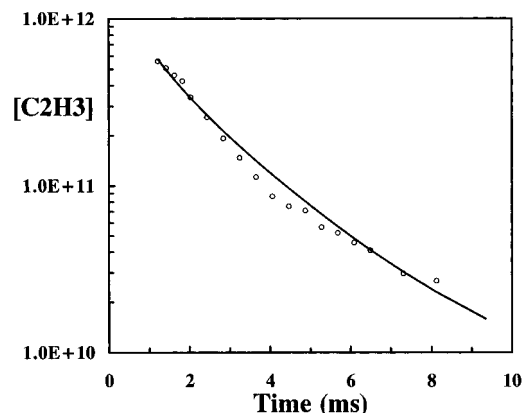


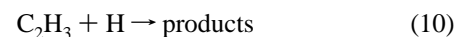
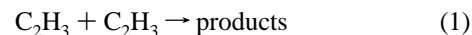
Figure 1. Plot of $[\text{C}_2\text{H}_3]$ (open circles) vs reaction time. $[\text{F}]_0 = 5.28 \times 10^{12} \text{ molecules cm}^{-3}$; $[\text{C}_2\text{H}_4]_0 = 1.57 \times 10^{14} \text{ molecules cm}^{-3}$. Solid line is the FACSIMILE numerical fit using the reaction scheme given in Table 1 with $k_{1b} = 1.38 \times 10^{-10} \text{ cm}^3 \text{ molecule}^{-1} \text{ s}^{-1}$.

determined as a fitted parameter to each of the observed $[\text{CH}_3]$ temporal profiles using the FACSIMILE program.⁴³ The important reactions used and their respective rate constants are listed in the lower half of Table 1. For association reactions, the rate constants have been calculated at $P = 1$ Torr He. The initial values of $[\text{F}]$, $[\text{C}_2\text{H}_4]$, and undissociated $[\text{F}_2]$ were needed as input data. The results showed that the methyl source rate was proportional to $[\text{F}]_0$. Thus, it was parameterized as a function of $[\text{F}]_0$.

Materials. Helium (99.999%, Air Products) was dried by passage through a trap held at $T = 77 \text{ K}$ before entering the flow system. F_2 (99.9%, Cryogenic Rare Gases, 5% in He), CH_4 (99.9995%, MG Industries), and Cl_2 (99.9%, Matheson, 3.5% in He) were used as provided without further purification. C_2H_2 (99.6%, Matheson), C_2H_4 (99.999%, Matheson), CF_4 (99%, Matheson), and C_4H_6 (1,3-butadiene) (99.8%, Matheson Research Grade) were degassed using repeated freeze–pump–thaw cycles at liquid nitrogen temperature.

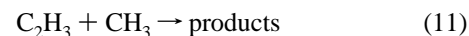
Results

A. Kinetics. Because the vinyl source generated H ($[\text{H}]_0 = 1.86[\text{C}_2\text{H}_3]_0$) within 1 ms, rate coefficients for the vinyl self reaction could not be measured under purely second-order conditions. The initial net C_2H_3 signal decay profile is expected to be dominated by



$$k_{10}(T=298 \text{ K}) = 1.1 \times 10^{-10} \text{ cm}^3 \text{ molecule}^{-1} \text{ s}^{-1} \text{ (ref 19)}$$

Hence, k_1 was measured under mixed first- and second-order conditions by monitoring the decay of C_2H_3 as a function of contact time. Fortuitously, CH_3 (generated as a secondary product from the C_2H_3 source) appears on a longer time scale after most of the C_2H_3 net signal has decayed. This reduces the consumption of C_2H_3 by CH_3 , even though the reaction of C_2H_3 with CH_3 is fast:

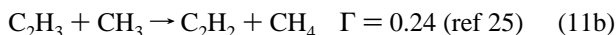
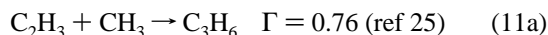
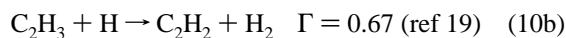
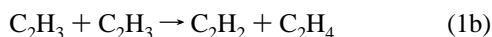


$$k_{11}(T=298 \text{ K}) = 1.5 \times 10^{-10} \text{ cm}^3 \text{ molecule}^{-1} \text{ s}^{-1} \text{ (refs 14, 25)}$$

Nonetheless, CH_3 chemistry was included in the kinetic analysis.

A typical C_2H_3 temporal profile observed at $m/z = 27$ is shown in Figure 1. Nonexponential decays were observed

except under conditions where $[F]_0$ and hence $[C_2H_3]_0$ were low, i.e., $[C_2H_3]_0 < 3.0 \times 10^{11}$ molecule cm^{-3} . The initial fast component of the decay became faster when $[F]_0$ was increased but was independent of variations in $[C_2H_4]_0$, and of the F atom precursors $[F_2]_0$ or $[CF_4]_0$, as long as $[F]_0$ was constant. On the basis of the above observations, we conclude that the mechanism for C_2H_3 decay is as follows:



$C_2H_3 \rightarrow$ decay by first-order processes including radial and axial diffusion and wall reactions (12)

A substantial fraction (~42%) of the observed initial C_2H_3 radical decay is due to the fast reaction 10, since $[H]_0 = 1.86[C_2H_3]_0$. Reaction 11 contributes very little to the initial C_2H_3 decay rate.

Possible contributions from secondary reactions reforming C_2H_3 ,



$$k_{13}(T=298 \text{ K}, P=1 \text{ Torr He}) = 8.8 \times 10^{-15} \text{ cm}^3 \text{ molecule}^{-1} \text{ s}^{-1} \text{ (ref 45)}$$

are negligible (<1%) under the conditions of both the CH_3 rise and C_2H_3 decay experiments. Results from experiments using CF_4 as the F atom precursor were identical to those that used F_2 . This indicates that consumption of C_2H_3 by reaction with the residual undissociated F_2



is negligible. However, F is regenerated from the residual F_2 on a slow but non-negligible time scale by



$$k_{15}(T=298 \text{ K}, P=1 \text{ Torr He}) = 2.5 \times 10^{-12} \text{ cm}^3 \text{ molecule}^{-1} \text{ s}^{-1} \text{ (ref 47)}$$

$$k_{16}(T=298 \text{ K}, P=1 \text{ Torr He}) = 1.0 \times 10^{-12} \text{ cm}^3 \text{ molecule}^{-1} \text{ s}^{-1} \text{ (ref 48)}$$

Therefore, reactions 15 and 16 were included in the program when modeling experiments that used F_2 as the F atom precursor.

Finally, k_1 was determined by a one-parameter fitting of the net C_2H_3 signal decays to a numerical simulation (FACSIMILE program)⁴³ of the reaction system. The mechanism consisted of reactions given in Table 1. Many of the reactions given in Table 1 are of minor consequence to k_1 determination, especially the CH_3 reactions. Neglect of the CH_3 reaction changes the derived value for k_1 by less than 2%.

TABLE 2: Summary of Rate Data for the C_2H_3 Self Reaction at $T = 298 \text{ K}^c$

atomic F precursor	$[F]_0/10^{12}$ molecule cm^{-3}	$[C_2H_3]_0/10^{11}$ molecule cm^{-3}	k_{12} s^{-1}	k_1^a 10^{-10} cm^3 molecule $^{-1}$ s^{-1}
F_2	2.60	9.1	100	$2.40 < 2.48 < 2.55$
F_2	7.16	25.1	140	$1.20 < 1.26 < 1.33$
F_2	8.18	28.6	92	$1.09 < 1.17 < 1.26$
F_2	5.17	18.1	92	$0.91 < 1.04 < 1.20$
F_2	7.43	26.0	92	$0.88 < 0.98 < 1.08$
F_2	5.28	18.5	94	$1.15 < 1.20 < 1.25$
F_2	8.14	28.5	94	$1.53 < 1.62 < 1.71$
F_2	5.28	18.5	73	$1.30 < 1.38 < 1.45$
F_2	6.72	23.5	73	$0.92 < 0.99 < 1.05$
F_2	5.49	19.2	76	$1.60 < 1.73 < 1.86$
F_2	2.96	10.4	76	$1.64 < 1.74 < 1.84$
CF_4	1.10	3.8	66	$0.71 < 0.79 < 0.88$
CF_4	2.24	7.8	66	$1.89 < 1.97 < 2.05$ (1.41 ± 0.48) ^b

^a 95% confidence levels on either side of central value. ^b Mean value of k_1 . Statistical error only at 1 standard deviation. ^c $[C_2H_4]_0 = (0.5-1.6) \times 10^{14}$ molecules cm^{-3} . Nominal pressure = 1 Torr (He).

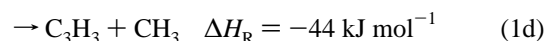
The first-order C_2H_3 loss rate, k_{12} , and the mass spectrometer signal calibration were determined in separate experiments using low $[F]_0$. The slope of the observed first-order decay equals $k_{10}[H] + k_{12}$, while the intercept at $t = 0$ yields $[C_2H_3]_0$ and hence the C_2H_3 signal calibration. These first-order C_2H_3 decay experiments were performed either just before or just after the mixed C_2H_3 decay experiments. The daily average value of k_{12} (66–140 s^{-1}) was used for the program input; the mean experimental value measured under the present conditions was 89 s^{-1} . This value is comparable to the C_2H_3 wall loss rates of 80 and 96 s^{-1} measured in our previous vinyl kinetic studies.^{18,19} The other input parameter was the initial atomic fluorine concentration, $[F]_0$, which was determined in the separate aforementioned atomic F titration experiments. Finally, the mixed decay experiments were performed and simulated under the following conditions: $T = 292-298 \text{ K}$, $P = 1.00-1.05 \text{ Torr}$, $[F]_0 = (1.1-8.2) \times 10^{12}$ molecule cm^{-3} , $[C_2H_4]_0 = (0.5-1.6) \times 10^{14}$ molecule cm^{-3} , and $[C_2H_3]_0 = (0.4-2.9) \times 10^{12}$ molecule cm^{-3} .

Table 2 summarizes the experimental conditions, the measured k_{12} values, and modeling results for the 13 independent kinetic experiments performed. The values of k_1 obtained in the simulations are given with their 95% confidence levels. The resulting mean value for $k_1(298 \text{ K})$ with 1σ statistical uncertainty is $k_1 = (1.41 \pm 0.48) \times 10^{-10} \text{ cm}^3 \text{ molecule}^{-1} \text{ s}^{-1}$. To allow for systematic errors, mostly in $[C_2H_3]_0$ and k_{10} , we add an additional $\pm 10\%$ uncertainty to obtain the rate constant

$$k_1(T=298 \text{ K}) = (1.41 \pm 0.60) \times 10^{-10} \text{ cm}^3 \text{ molecule}^{-1} \text{ s}^{-1}$$

where k_1 is defined by $d[C_2H_3]/dt = 2k_1[C_2H_3]^2$.

B. Products. In order to determine the product branching ratios, measurements were made on the absolute yields of the expected products, both acetylene ($m/z = 26$) and *E*-1,3-butadiene ($m/z = 54$). Because ethylene was used as a precursor for vinyl production, it was present in concentrations too large to accurately obtain a product yield measurement. Experiments were also performed to detect C_3H_3 ($m/z = 39$) and C_4H_5 ($m/z = 53$), which could result from two possible exothermic channels:^{6,24,49}



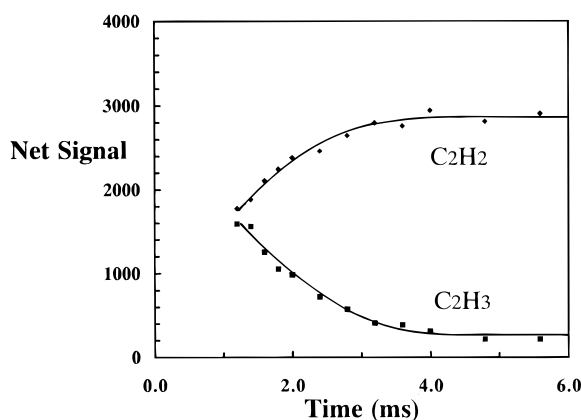


Figure 2. Plot of net C_2H_2 signal (solid diamonds) and net C_2H_3 signal (solid squares) vs reaction time. $[F]_0 = 4.24 \times 10^{12}$ molecules cm^{-3} ; $[C_2H_4]_0 = 1.53 \times 10^{14}$ molecules cm^{-3} .

Typical conditions used were similar to those in the kinetic decay experiments. Initial vinyl concentrations were $[C_2H_3]_0 = (1.3-2.1) \times 10^{12}$ molecule cm^{-3} , and this ensured completion of all vinyl reactions within 10 ms as well as formation of detectable levels of products. Both F_2 and CF_4 were used as F atom precursors. The product yields were determined by monitoring product signals as a function of distance (reaction time). The product profiles consisted of an increasing signal that leveled off, indicating that the C_2H_3 self reaction had gone to completion.

At ionization energy of 11.5 eV, C_4H_6 was not detected as a product of reaction 1, since the net $m/z = 54$ signal was not statistically above the background signal. Calibration of the mass spectrometer with a reference mixture of 1,3-butadiene showed that it was detectable at a concentration of 1.0×10^9 molecule cm^{-3} at $S/N = 1$. An ionization energy of 11.5 eV is above the ionization energy for all C_4H_6 isomers including the following: 1,3-butadiene ($CH_2=CH-CH=CH_2$), IE = 9.08 eV; 1,2-butadiene ($CH_2=C=CH-CH_3$), IE = 9.03 eV; cyclobutene, IE = 9.43 eV; 1-butyne ($CH\equiv C-CH_2-CH_3$), IE = 10.19 eV; 2-butyne ($CH_3-C\equiv C-CH_3$), IE = 9.59 eV.⁵⁰ Thus, a conservative upper limit for the fractional product branching ratio Γ_{1a} would be ≤ 0.01 .

Neither C_4H_5 nor C_3H_3 was detected as products of reaction 1. Experiments using 11.5 eV ionization energy showed that the respective $m/z = 53$ and $m/z = 39$ signals were not statistically above the background signal. Further evidence for the absence of propargyl radical, C_3H_3 , was obtained by trying to detect 1,3-cyclopentadiene, C_5H_6 , at $m/z = 66$. C_5H_6 has been observed²⁴ as a major product in flow tubes containing high concentrations of vinyl radical at $T = 623$ K. It results from



At ionization energy of 12.0 eV, C_5H_6 (IE = 8.56 eV, ref 50) was not detected as a product of reaction 17, since the net $m/z = 66$ signal was not statistically above the background signal. Thus, the only product detected was acetylene.

As shown in Figure 2, a simultaneous decay of net vinyl signal to background and a rise of net acetylene signal was observed. The magnitude of the acetylene product signal was calibrated using a range of appropriate known concentrations of the reference acetylene under flow conditions similar to those in the product experiments. Acetylene is also a product of the $H + C_2H_3$ reaction. Therefore, numerical modeling (with the same program, reaction set, and kinetic parameters as described

TABLE 3: Ratio of $[C_2H_2]$ Formed from the Combined $C_2H_3 + C_2H_3$ and $C_2H_3 + H$ Reactions to the Initial Vinyl Radical Concentration $[C_2H_3]_0$ ^b

atomic F precursor	$[C_2H_3]_0$	$[C_2H_2]_\infty$	$[C_2H_2]_\infty/[C_2H_3]_0$
CF_4	2.08×10^{12}	1.42×10^{12}	0.68
CF_4	1.27×10^{12}	7.07×10^{11}	0.49
F_2	1.48×10^{12}	9.45×10^{11}	0.55
F_2	1.30×10^{12}	7.39×10^{11}	0.51
F_2	1.48×10^{12}	1.15×10^{12}	0.70
F_2	1.75×10^{12}	1.36×10^{12}	0.78
F_2	1.27×10^{12}	1.07×10^{12}	0.84
			$(0.65 \pm 0.14)^a$

^a Mean value. Statistical error only at 1 standard deviation. Modeled value with equal contribution from $C_2H_3 + C_2H_3$ and $C_2H_3 + H$ reactions is 0.59. ^b $[C_2H_4]_0 = (1.2-1.5) \times 10^{14}$ molecules cm^{-3} . Nominal pressure = 1 Torr (He).

above in the Kinetics section) was used to predict the total acetylene produced within the flow tube. Even assuming the maximum 100% disproportionation for vinyl self reaction (with $k_{1b} = 1.41 \times 10^{-10}$ cm^3 molecule⁻¹ s⁻¹), the experimentally measured $[C_2H_2]$ was on the average about 10% greater than the modeled $[C_2H_2]$. The modeling results further showed that the C_2H_3 self reaction and the $C_2H_3 + H$ reaction contributed in equal amounts to the C_2H_2 generation. Table 3 summarizes the results of seven separate experiments at different values of initial vinyl radical concentration $[C_2H_3]_0$ and using different sources of atomic fluorine (microwave discharge of F_2/He and CF_4/He mixtures). The average value of the observed ratio $[C_2H_2]$ formed from the vinyl reactions at $t \approx 4-6$ ms (all C_2H_3 reacted) to the initial vinyl radical concentration $[C_2H_3]_0$ is 0.65 ± 0.14 , where the quoted error is statistical at 1 standard deviation. Assuming the maximum C_2H_2 yield of 0.50 from the disproportionation reaction $2C_2H_3 \rightarrow C_2H_2 + C_2H_4$ and a C_2H_2 product yield of 0.67¹⁹ from the $C_2H_3 + H$ reaction, the expected $[C_2H_2]/[C_2H_3]_0$ ratio is the average of these yields or 0.59. The agreement between observed and modeled values for $[C_2H_2]/[C_2H_3]_0$ within experimental uncertainty strongly suggests that C_2H_2 and C_2H_4 are the exclusive products of reaction 1. This is of course also consistent with our lack of observation of the combination product 1,3-butadiene.

One possible explanation for the observed $[C_2H_2]$ being slightly higher than the model prediction is that acetylene is generated in a vibrationally excited state and therefore has a higher ionization cross section than thermalized C_2H_2 .^{24,51} Vibrationally excited C_2H_2 would have a lower ionization energy than that for thermalized C_2H_2 . However, ionization threshold experiments resulted in the same ionization energy for both reaction-generated C_2H_2 and reagent C_2H_2 . Even if vibrationally excited C_2H_2 were initially formed in the flow tube, it would be expected to be collisionally relaxed before being sampled by the mass spectrometer.

Discussion

The three measured k_1 values at $T = 298$ K are summarized in Table 4. The results of the relative rate studies based on complex analysis have been neglected. Besides our direct, modeled k_1 determination, the list includes two direct but not absolute measurements^{14,22} and one direct absolute measurement.²³ Our k_1 value overlaps with the total k_1 rate in both of the high-pressure studies. At lower pressures, MacFadden and Currie²³ observed mainly a disproportionation channel, but their reported k_1 value is considerably lower than the other results in Table 4. Their lower value could be due to their lower pressure or to uncertainties in the reaction cell temperature after the flash as well as uncertainties in the determination of the initial vinyl radical concentration.

TABLE 4: Comparison of the Rate Constants Measured or Estimated for the C₂H₃ Self Reaction at T = 298 K

pressure He (Torr)	k_1^a	technique ^b	ref
1.0	14.1 ± 6.0	DF-MS	this work
100	14.4 ± 3.5	LP-UVA	14
400	10.0 ± 2.5	LP-UVA	22
0.14–0.20 ^c	0.53 ± 0.05	FP-MS	23

^a Rate coefficients given in units of 10⁻¹¹ cm³ molecule⁻¹ s⁻¹. ^b DF-MS, discharge flow mass spectrometry; LP-UVA, laser photolysis UV absorption; FP-MS, flash photolysis mass spectrometry. ^c Pressure of mixture 25–75% divinyl ether in Ne.

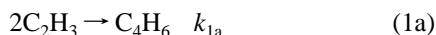
The measurements of k_1 summarized in Table 4 have been made over a wide range of pressures: 0.14–0.2 Torr in ref 23, 1.0 Torr He in our study, 100 Torr He in ref 14, and 400 Torr He in ref 22. For our low-pressure experiments, the rate constant value, $k_1 = (1.41 \pm 0.60) \times 10^{-10}$ cm³ molecule⁻¹ s⁻¹, approximates the rigid sphere collisional rate of 1.0×10^{-10} cm³ molecule⁻¹ s⁻¹. This suggests a near zero activation energy for the reaction. The higher pressure studies^{14,22} reveal that the combination channel is the dominant pathway under these conditions. Considering our data and the recent studies of Fahr and colleagues,^{14,22,25} we conclude that although the vinyl self reaction total rate constant can be considered pressure independent, the product branching ratio cannot.

A. Mechanistic Considerations. The pressure dependencies of the apparent decay of C₂H₃, k_{tot} , and the ratio of products, $R = [\text{C}_2\text{H}_2]/[\text{C}_4\text{H}_6]$, provide important information on the mechanism for the overall branching. As before, k_{tot} is defined as

$$k_{\text{tot}} = -(\text{d}[\text{C}_2\text{H}_3]/\text{d}t)/(2[\text{C}_2\text{H}_3]^2)$$

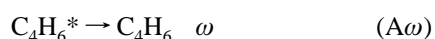
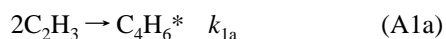
A mechanism must be found to fit the observations that k_{tot} is independent of pressure and R is pressure dependent. The presentation of four mechanisms and their steady state solutions follow.

The simplest mechanism, corresponding to two elementary processes,



gives $k_{\text{tot}} = k_{1a} + k_{1b}$ and $R = [\text{C}_2\text{H}_2]/[\text{C}_4\text{H}_6] = k_{1b}/k_{1a}$. This mechanism does not fit the experimental observations, since all these quantities are independent of pressure.

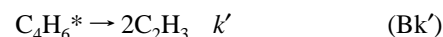
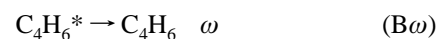
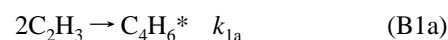
Pressure dependence can easily be introduced, since the combination of two C₂H₃ radicals produces a highly vibrationally excited (chemically activated) 1,3-butadiene that can either be collisionally stabilized (ω is the collision frequency, which is linearly dependent upon pressure) or undergo unimolecular reaction. For simplicity, in this section, we assume that the chemically activated 1,3-butadiene is formed with a δ function energy distribution at the average thermal energy and that collisions are strong, i.e., a single collision removes sufficient energy so that unimolecular reaction is quenched. Thus, reaction 1a shown above, which was considered to be a single step, would be replaced by the series of reactions



For this mechanism (designated as “A”) $k_{\text{tot}} = k_{1b} + k_{1a}\{1 -$

$k'/(k' + \omega)\}$ and $R = (k_{1b}/k_{1a})(1 + k'/\omega)$. For the case that $\omega \gg k'$, i.e., the high-pressure limit, these equations reduce to those for the simplistic mechanism: $k_{\text{tot}} = k_{1a} + k_{1b}$ and $R = k_{1b}/k_{1a}$. As shown below, the pressures (1 Torr = 1.5×10^7 collisions/s) in the present experiments correspond to the high-pressure limit, since $k' \approx 10^3$ s⁻¹ (see next section for calculation). However, in the low-pressure limit ($\omega < k'$), there is no stabilization of 1,3-butadiene. Only the reverse of the combination reaction, k_{1a} occurs, so $k_{\text{tot}} = k_{1b}$ and $R \rightarrow \infty$, i.e., only disproportionation (k_{1b}) is observed. Thus, this mechanism does provide a pressure independence for k_{tot} as is experimentally observed but does not exhibit a pressure dependence for R in the pressure regime of the experiments. However, there is a pressure dependence for R at lower pressure, i.e., in the pressure range of 10⁻³ to 10⁻⁴ Torr.

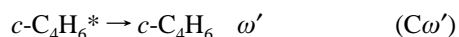
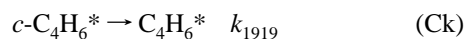
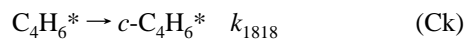
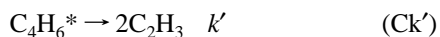
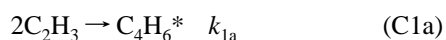
An improvement on this mechanism (henceforth designated as B) would be to add a unimolecular step that directly produces C₂H₂ so that reaction 1a is replaced by the sequence of reactions



For this mechanism, $k_{\text{tot}} = k_{1b} + k_{1a}\{1 - k'/(k' + k + \omega)\}$ and $R = \{k_{1b}/k_{1a} + k/(k' + k + \omega)\}/\{\omega/(k' + k + \omega)\}$. Since there are now two sources for C₂H₂ (reactions 1b and Bk), it is convenient to define a new quantity: $F = [\text{C}_2\text{H}_2(1b)]/[\text{C}_2\text{H}_2(\text{tot})]$ where $[\text{C}_2\text{H}_2(\text{tot})] = [\text{C}_2\text{H}_2(1b)] + [\text{C}_2\text{H}_2(1a)]$. Although F cannot be experimentally determined, it is useful for determining the importance of the effective branching between reactions B1a and 1b. As calculated in the next section, $k \gg k'$ so that in the low-pressure limit $k_{\text{tot}} = k_{1a} + k_{1b}$. In the high-pressure limit k_{tot} is the same as in mechanism “A”, i.e., $k_{1a} + k_{1b}$. R has the same high-pressure limit (k_{1b}/k_{1a}) as in mechanism “A”, while in the low-pressure limit $R \rightarrow \infty$. The limiting values for F in the high- and low-pressure limits are 1 and $k_{1b}/(k_{1a} + k_{1b})$, respectively. For the present experiments, with $k \gg k'$, k_{tot} will not be pressure dependent while R will be; the pressure dependence will occur when $\omega \approx k$. Although this mechanism provides the right pressure dependence, it has one major deficiency: there have not been any reports of the unimolecular decomposition of 1,3-butadiene to directly produce C₂H₂ and C₂H₄; only the decomposition producing vinyl radicals has been reported.⁵²

Mechanism “C” provides a more feasible precursor for C₂H₂ and C₂H₄. In this mechanism cyclobutene (*c*-C₄H₆) is formed by the isomerization (k_{18}) of chemically activated 1,3-butadiene. The cyclobutene can (i) isomerize (k_{19}) to 1,3-butadiene,⁵³ (ii) be collisionally stabilized (ω), or (iii) decompose (k) to C₂H₂ and C₂H₄. Although the decomposition of cyclobutene has not been observed, the decomposition of cyclobutane to ethylene has been and Arrhenius parameters reported.⁵⁴ Both reactions are symmetry forbidden.⁵⁵ The critical energy for the decomposition of cyclobutane is ~60 kcal/mol.⁵⁴ Since the isomerization of cyclobutene has a critical energy of ~32 kcal/mol,⁵⁴ it is not expected that the decomposition to C₂H₂ would be competitive for systems involving thermal activation. However, in externally activated systems where the energy is in excess of both critical energies, both processes are possible. The importance of these two processes will be determined by their respective excess energies and frequencies for the activated

complexes. The following steps make up mechanism "C":



The expressions for k_{tot} , R , and F for this mechanism are given by

$$k_{\text{tot}} = k_{1b} + k_{1a}(1 - k'(k_{19} + k + \omega)/D)$$

$$R = \{k_{1b}/k_{1a} + k_{18}k/D\} / \{(k_{19} + k + \omega)\omega/D\}$$

$$F = 1 / (1 + (k_{1a}/k_{1b})k_{18}k/D)$$

where $D = k'k_{19} + k'k + k_{18}k + \omega(k' + k_{18} + k_{19} + k) + \omega^2$. The limiting pressure dependencies correlate with what is experimentally observed, and the transition pressure from the limiting high- and low-pressure limits is in the regions where there is no experimental data. At low pressure there is no stabilization, so the 1,3-butadiene and cyclobutene concentrations are zero, $R \rightarrow \infty$, and $F = k_{1b}/(k_{1a} + k_{1b})$. At high pressure only 1,3-butadiene from the (1a) channel is observed, so $R = k_{1b}/k_{1a}$ and $F = 1$. In the transition region both 1,3-butadiene and cyclobutene are present. When $k_{19} > k$ and $\omega \approx k_{19}$, then the ratio of 1,3-butadiene to cyclobutene is $\sim k_{19}/k_{18}$, i.e., a pseudo equilibrium is established. The values of k_{18} and k_{19} produce $[\text{C}_4\text{H}_6^*]/[c\text{-C}_4\text{H}_6^*] \approx 10^2$. k_{tot} is independent of pressure over the experimental pressure range, while both R and F will be pressure dependent. As contrasted with R , F has a well-defined value for the high- and low-pressure limits. This mechanism indicates that cyclobutene should be observed in the 1–100 Torr range, i.e., when $\omega \approx k$. This mechanism can be discarded if no cyclobutene is experimentally observed in the intermediate pressure region.

B. Details of Calculated Quantities. The feasibility of mechanism "C" can be tested by performing calculations with a reasonable set of kinetic parameters and assumptions. Four sets of quantities must first be determined before the observables (k_{tot} , $[\text{C}_2\text{H}_2]$, $[\text{C}_4\text{H}_6]$, and R) can be calculated: (1) branching ratio k_{1b}/k_{1a} , (2) collision frequency, (3) energy distribution function for 1,3-butadiene, and (4) the energy dependent microscopic unimolecular rate coefficients (k' , k , k_{18} , and k_{19}). For the present calculations we will use the value of $k_{1b}/k_{1a} = 0.2$ as supported by the high-pressure experiments^{14,22} listed in Table 4. By use of a collision diameter of 3.4 Å, the collision frequency of helium with the C_4H_6 species at 25 °C is $1.5 \times 10^7 p$ (collisions/s)⁵⁶ where p is the pressure in Torr. Although helium is a weak collision partner, the use of an effective collision frequency,⁵⁷ ω_{eff} , has been successfully used to calculate the pressure dependence. In this case ω_{eff} is replaced by $\beta\omega$; for helium $\beta \approx 0.2$.⁵⁷ Alternatively, an energy transfer probability model could be used in the master equation formulation⁵⁶ so that the observed quantities could be calculated. For the present objectives this was not necessary.

C. 1,3-Butadiene Energy Distribution. Owing to thermal energy of the vinyl radicals, the 1,3-butadiene also has an energy distribution, $f(E)$, that is different from the Boltzmann distribution at ambient temperature. The energy distribution for an association reaction, as determined by detailed balance,⁵⁸ is given by

$$f(E) dE = k'(E)B(E) dE / \int k'(E)B(E) dE$$

where $B(E)$, the Boltzmann distribution, is given by $B(E) = N(E) e^{-E/RT} dE / \int N(E) e^{-E/RT} dE$ and $N(E)$ is the density of rotational–vibrational energy states for the reactant. The normalization of $f(E)$ requires integration from E_{min} , the minimum excitation energy, to infinity. The energy dependent rate coefficient for the decomposition of 1,3-butadiene to vinyl radicals is given by $k'(E)$. Calculation of this quantity is given below.

D. Microscopic Rate Coefficients. The unimolecular rate coefficients, $k'(E)$, $k(E)$, $k_{18}(E)$, and $k_{19}(E)$, can be calculated from the Marcus expression^{56,59} for $k(E)$:

$$k(E) = c(1/h) \sum P(\epsilon) / N(E)$$

$\sum P(\epsilon)$ is the sum of rotational–vibrational states for the transition state, $N(E)$ was defined earlier, and c is a constant that depends on the adiabatic partition functions, symmetry numbers, and reaction path degeneracy. We have set $c = 1$, since for the reactions considered here, $c \approx 1$. The energetics and vibrational frequencies for the reactant and transition state are necessary to calculate $N(E)$ and $\sum P(\epsilon)$. Heats of reaction and reported Arrhenius parameters (values for the activation energies and A factors) were used for the calculations that follow. Previously published frequencies^{60–62} or modifications of them were used so that the model would reproduce reported Arrhenius A factors within a factor of 2 for the specific or analogous reactions. Previously established equations were used to calculate E_a and A .⁵⁴ No attempt was made to refine the parameters used in these calculations, since only semiquantitative behavior was sought. A tabulation of these quantities and the rate coefficients at an energy equal to the average energy of reacting 1,3-butadiene is given in Table 5.

An energy level diagram defining the respective energies is presented in Figure 3. The chemically activated 1,3-butadiene is formed with approximately 100 kcal/mol of internal energy, which is available for reaction. Thus, the minimum energy for the decomposition of 1,3-butadiene is 100 kcal/mol. The isomerization of 1,3-butadiene to cyclobutene is endoergic by ~ 10 kcal/mol; since E_a for the isomerization of cyclobutene is ~ 32 kcal/mol, the isomerization of 1,2-butadiene is ~ 42 kcal/mol. The A factor for the isomerization of 1,3-butadiene to cyclobutene can be calculated from ΔS^\ddagger for the isomerization reaction.

E. Calculated Quantities. Values for k_{tot} , R , and F were calculated from the following equations:

$$k_{\text{tot}} = \int \{k_{1b} + k_{1a}(1 - k'(E)(k_{19}(E) + k(E) + \omega)/D(E))\} f(E) dE$$

$$R = \int \{k_{1b}/k_{1a} + k_{18}(E)k(E)/D(E)\} f(E) dE / \int \{(k_{19}(E) + k(E) + \omega)\omega/D(E)\} f(E) dE$$

$$F = 1 / \int \{1 + (k_{1a}/k_{1b})k_{18}(E)k(E)/D(E)\} f(E) dE$$

where $D(E) = k'(E)k_{19}(E) + k'(E)k(E) + k_{18}(E)k(E) + \omega[k'(E) + k_{18}(E) + k_{19}(E) + k(E)] + \omega^2$.

The results of calculations for the various mechanisms are shown in Figures 4 and 5. Since Bk is not known, we have set

TABLE 5: Reported Kinetic Parameter Values and Values Used in the Calculations

reaction	reported values		values from assumed models used in calculations			
	A (s ⁻¹)	E _a (kcal/mol)	A (s ⁻¹)	E _a (kcal/mol)	E ₀ ^a (kcal/mol)	k(⟨E⟩) ^b (s ⁻¹)
Ck ₁₈	2.0 × 10 ^{12c}	42.2	2.0 × 10 ^{12d}	41.5	42	5.9 × 10 ⁸
Ck ₁₉	2.5 × 10 ^{13e}	32.5	1.6 × 10 ^{13f}	32.3	32	5.3 × 10 ¹⁰
Ck'	2.0 × 10 ^{17g}	94	1.3 × 10 ^{17h}	102.2	100	9.1 × 10 ²
Ck	4.0 × 10 ¹⁵ⁱ	62.5	3.0 × 10 ^{15j}	61.0	60	1.4 × 10 ¹⁰

^a E₀ is the energy required to excite reactant in its zero-point state to the transition state in its zero-point state. ^b For comparative purposes k(⟨E⟩) is set such that ⟨E⟩ is the average energy of 1,3-butadiene formed by reaction 1a, ~104 kcal/mol above the zero-point energy of 1,3-butadiene. ^c Calculated from the equations A₁₈ = A₁₉ e^{ΔS[‡]/RT} and E_a(18) = E_a(19) + ΔE⁰ for C₄H₆ → c-C₄H₆. ΔH⁰_{298 K} = 9.7 kcal/mol and ΔS⁰_{298 K} = -3.6 cal/K·mol for unimolecular reactions ΔE⁰ = ΔH⁰. Values taken from ref 54. ^d Vibrational frequencies for 1,3-butadiene taken from ref 61 and those for the transition state taken from ref 60. ^e Taken from ref 54. ^f Vibrational frequencies for cyclobutene and the transition state taken from ref 60. ^g Estimated from the A factor cited in ref 54 for the decomposition of butane to give two ethyl radicals. ^h Vibrational frequencies for 1,3-butadiene taken from ref 60 and the transition state frequencies estimated by using frequencies for vinyl as reported in ref 62. ⁱ Assumed to be the same Arrhenius parameters as for the decomposition of cyclobutane as cited in ref 54. ^j Vibrational frequencies for cyclobutene taken from ref 60 and the transition frequencies determined by reducing C-C stretches and bending modes to give an A factor comparable to that cited in ref 54 for the decomposition of cyclobutane.

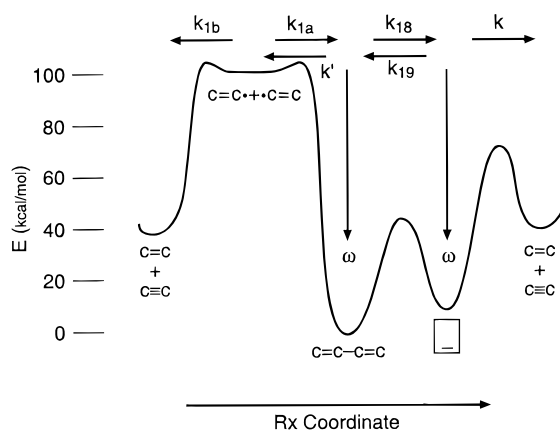


Figure 3. Potential energy profile for mechanism "C" as described in text.

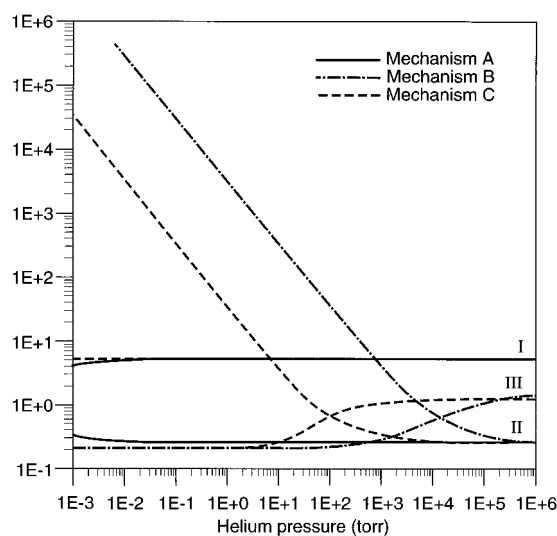


Figure 4. Plots of (I) k_{10}/k_{1b} ($k_{1b} = 2 \times 10^{-11} \text{ cm}^3 \text{ molecule}^{-1} \text{ s}^{-1}$) vs helium pressure for mechanisms "A", "B", and "C", (II) R ($[C_2H_2]/[C_4H_6]$) vs helium pressure for mechanisms "A", "B", and "C", and (III) F ($[C_2H_2(1b)]/\{[C_2H_2(1b)] + [C_2H_2(1a)]\}$) vs helium pressure for mechanism "B" and "C". Note that this is the measured helium pressure, not the effective pressure.

it equal to Ck for these comparisons. Figure 4 illustrates that the falloff of k_{10} with decreasing helium pressure starts at a helium pressure of $\sim 5 \times 10^{-2}$ Torr for mechanism "A", much lower than what is observed for "B". The dependence of R for "B" and "C" on the helium pressure is also shown in Figure 4. R rises at a higher pressure for "B" than it does for "C". It starts rising at a helium pressure of $\sim 1 \times 10^5$ Torr for "B", while for "C" it starts at about 1000 Torr. The pressure at which

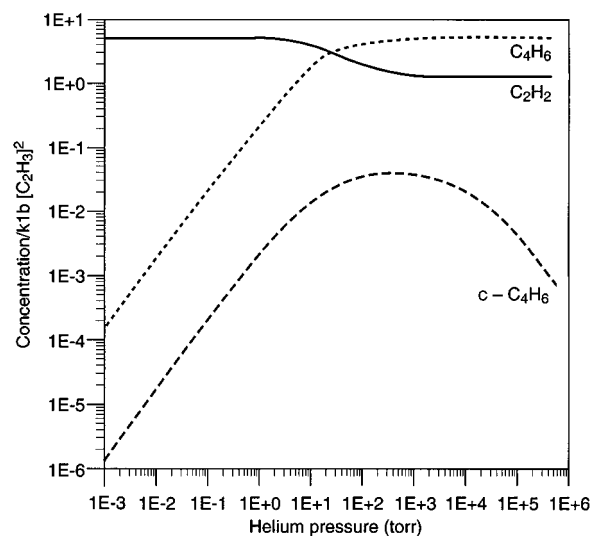


Figure 5. Plots of $[C_2H_2]/k_{1b}[C_2H_3]^2$, $[C_4H_6]/k_{1b}[C_2H_3]^2$, and $[c-C_4H_6]/k_{1b}[C_2H_3]^2$ vs helium pressure for mechanism "C". Note that this is the measured helium pressure, not the effective pressure.

the increase starts is governed by the parameters used for Bk or Ck. The transition pressures for F are similar for mechanisms "B" and "C".

The pressure dependence for the stable products (C_2H_2 , C_4H_6 , and $c-C_4H_6$) in mechanism "C" is shown in Figure 5. At low pressure C_2H_2 is the dominant product; C_2H_2 is produced both by disproportionation (1b) and the decomposition of the chemically active C_4H_6 species formed by the combination (1a) reaction. As the pressure increases, energy is removed from the C_4H_6 species so that decomposition is quenched, i.e., C_2H_2 decreases. Before the chemically activated 1,3-butadiene is totally quenched, there is a pseudoequilibrium between 1,3-butadiene and cyclobutene; $[C_4H_6]/[c-C_4H_6] \approx 10^2$. With a further increase in pressure the isomerization is quenched and only C_4H_6 is formed and $[C_2H_2]/[C_4H_6] = k_{1b}/k_{1a}$.

Summary and Conclusions

The discharge-flow technique coupled with mass spectrometric detection has been used to study the self reaction of C_2H_3 at 298 K with a helium bath gas pressure of ~ 1 Torr. C_2H_3 was produced by the reaction of F with C_2H_4 . The formation reaction also produced H, which can react with C_2H_3 and C_2H_4 to produce C_2H_2 and CH_3 , respectively. Contributions from these reactions were adequately modeled. The time profiles for C_2H_3 , C_2H_2 , and CH_3 were experimentally determined and modeled with the FACSIMILE program; 1,3-butadiene and other C_3 , C_4 , and C_5 products were not observed. The importance of

secondary reactions was assessed; CH₃ is generated on a longer time scale than C₂H₃. The rate coefficient for the combination of C₂H₃ was determined to be $(1.41 \pm 0.60) \times 10^{-10}$ cm³ molecule⁻¹ s⁻¹ in the 1 Torr region. This value is close to the gas kinetic collision rate. Earlier studies at higher pressures (>100 Torr) report a similar rate coefficient, but both 1,3-butadiene and C₂H₂ were observed.

Various mechanisms involving unimolecular isomerizations and/or decompositions have been tested using steady state RRKM calculations. The observed pressure independence for $k_1 (= k_{1a} + k_{1b})$ and the pressure dependence for [C₂H₂]/[1,3-butadiene] suggests a mechanism where the chemically activated 1,3-butadiene unimolecularly reversibly isomerizes to cyclobutene. At low pressures the chemically activated cyclobutene can undergo a symmetry forbidden retro 2 + 2 addition to produce C₂H₂ and C₂H₄. Thus, each C₂H₃ combination will produce a C₂H₂. At high pressures the chemically activated 1,3-butadiene is collisionally stabilized and [C₂H₂]/[1,3-butadiene] reaches a limiting value; no cyclobutene is produced at high pressure. Although this particular symmetry forbidden reaction has not been reported, it should have energetics similar to that of the decomposition of cyclobutane to give C₂H₄. The observed pressure dependence was reproduced by steady state RRKM calculations using vibrational frequency models and energetics reported for similar reactions. The cyclobutene decomposition is not expected to be observed in thermal systems, since the barrier is approximately 30 kcal/mol higher than for the isomerization to 1,3-butadiene. This contrasts with chemical activation systems in which energies are in excess of the critical energy for reaction; in thermal (collisional activation) systems the observed rate coefficient is dramatically reduced by the small Boltzmann factor for large critical energies. Future studies in which the pressure dependence in the transition region, 5–100 Torr, is determined will provide information on the validity of the proposed mechanism. The proposed mechanism predicts that at low pressure there is neither 1,3-butadiene nor cyclobutene, while at high pressures cyclobutene will not be observed. Thus, monitoring the pressure dependence of both 1,3-butadiene and cyclobutene will provide information on the proposed mechanism. The possibility of a concerted decomposition of 1,3-butadiene (mechanism "B") to directly give C₂H₂ and C₂H₄ will also be evaluated.

Acknowledgment. We thank Paul Romani for many helpful discussions. This work was supported by the NASA Planetary Atmospheres Research Program. R. Peyton Thorn thanks the National Academy of Sciences for the award of a research associateship.

References and Notes

- Romani, P. N.; Bishop, J.; Bézard, B.; Atreya, S. *Icarus* **1993**, *106*, 442.
- Allen, M.; Yung, Y. L.; Gladstone, G. R. *Icarus* **1992**, *100*, 527.
- Strobel, D. F. *Rev. Geophys. Space Phys.* **1975**, *13*, 372.
- Lellouch, E.; Romani, P. N.; Rosenqvist, J. *Icarus* **1994**, *108*, 112.
- Yung, Y. L.; Allen, M.; Pinto, J. P. *Astrophys. J., Suppl. Ser.* **1984**, *55*, 465.
- Lyons, J. R.; Yung, Y. L.; Allen, M. *Icarus*, submitted.
- (a) Herbst, E.; Leung, C. M. *Mon. Not. R. Astron. Soc.* **1986**, *222*, 689. (b) Herbst, E.; Leung, C. M. *Astrophys. J., Suppl. Ser.* **1989**, *69*, 271.
- Tsang, W.; Hampson, R. F. *J. Phys. Chem. Ref. Data* **1986**, *15*, 1087.
- Duran, R. P.; Amorebieta, V. T.; Colussi, A. J. *J. Phys. Chem.* **1988**, *92*, 636.
- Westmoreland, P. R.; Dean, A. M.; Howard, J. B.; Longwell, J. P. *J. Phys. Chem.* **1989**, *93*, 8171.
- Laufer, A. H.; Gardner, E. P.; Kwok, T. L.; Yung, Y. L. *Icarus* **1983**, *56*, 560.
- Timonen, R. *Ann. Acad. Sci. Fenn., Ser. A2* **1988**, *218*, 5.
- Fahr, A.; Laufer, A. H. *J. Phys. Chem.* **1988**, *92*, 7229.
- (a) Slagle, I. R.; Park, J.-Y.; Heaven, M. C.; Gutman, D. *J. Am. Chem. Soc.* **1984**, *106*, 4356. (b) Park, J.-Y.; Heaven, M. C.; Gutman, D. *Chem. Phys. Lett.* **1984**, *104*, 469.
- (a) Krueger, H.; Weitz, E. *J. Chem. Phys.* **1988**, *88*, 1608. (b) Russel, J. J.; Senkan, S. M.; Seetula, J. A.; Gutman, D. *J. Phys. Chem.* **1989**, *93*, 5184.
- Fahr, A.; Laufer, A. H.; Klien, R.; Braun, W. *J. Phys. Chem.* **1991**, *95*, 3218.
- Heinemann, P.; Hofmann-Sievert, R.; Hoyeremann, K. *Symp. (Int.) Combust., [Proc.]* **1986**, *21*, 865.
- Ibuki, T.; Takezaki, Y. *Bull. Chem. Soc. Jpn.* **1975**, *48*, 769.
- Payne, W. A.; Monks, P. S.; Nesbitt, F. L.; Stief, L. *J. Chem. Phys.*, in press.
- Monks, P. S.; Romani, P. N.; Nesbitt, F. L.; Scanlon, M.; Stief, L. *J. Geophys. Res.* **1993**, *98*, 17115.
- Monks, P. S.; Nesbitt, F. L.; Payne, W. A.; Scanlon, M.; Stief, L. J.; Shallcross, D. E. *J. Phys. Chem.* **1995**, *99*, 17151.
- Fahr, A. *Int. J. Chem. Kinet.* **1995**, *27*, 769.
- Fahr, A.; Monks, P. S.; Stief, L. J.; Laufer, A. H. *Icarus* **1995**, *116*, 415.
- Fahr, A.; Laufer, A. H. *J. Phys. Chem.* **1990**, *94*, 726.
- MacFadden, K. O.; Currie, C. L. *J. Chem. Phys.* **1973**, *58*, 1213.
- Kubitzka, C. Ph.D. Thesis, Technische Hochschule Darmstadt, Darmstadt, Germany, 1995.
- Fahr, A.; Braun, W.; Laufer, A. H. *J. Phys. Chem.* **1993**, *97*, 1502.
- Tickner, A. W.; Le Roy, D. J. *J. Chem. Phys.* **1951**, *19*, 1247.
- Sherwood, A. G.; Gunning, H. E. *J. Phys. Chem.* **1965**, *69*, 2323.
- Weir, N. A. *J. Chem. Soc.* **1965**, 6870.
- Takita, S.; Mori, Y.; Tanaka, I. *J. Phys. Chem.* **1968**, *72*, 4360.
- Szirovicza, L. *Int. J. Chem. Kinet.* **1985**, *17*, 117.
- Blush, J. A.; Chen, P. J. *J. Phys. Chem.* **1992**, *96*, 4138.
- Brunning, J.; Stief, L. *J. Chem. Phys.* **1986**, *84*, 4371.
- Nesbitt, F. L.; Payne, W. A.; Stief, L. *J. Phys. Chem.* **1988**, *92*, 4030.
- Clyne, M. A. A.; MacRobert, A. *Int. J. Chem. Kinet.* **1981**, *13*, 187.
- Brune, W. H.; Schwab, J. J.; Anderson, J. G. *J. Phys. Chem.* **1983**, *87*, 4503.
- Nesbitt, F. L.; Monks, P. S.; Scanlon, M.; Stief, L. *J. Phys. Chem.* **1994**, *98*, 4307.
- Slagle, I. R.; Gutman, D. *J. Phys. Chem.* **1983**, *87*, 1818.
- Appelman, E. H.; Clyne, M. A. A. *J. Phys. Chem.* **1975**, *71*, 2072.
- Marston, G.; Nesbitt, F. L.; Nava, D. F.; Payne, W. A.; Stief, L. *J. Phys. Chem.* **1989**, *93*, 5769.
- Lightfoot, P. D.; Pilling, M. J. *J. Phys. Chem.* **1987**, *91*, 3373.
- Nesbitt, F. L.; Marston, G.; Stief, L. *J. Phys. Chem.* **1990**, *94*, 4946.
- Stevens, P. S.; Brune, W. H.; Anderson, J. G. *J. Phys. Chem.* **1989**, *93*, 4068.
- Curtis, A. R.; Sweetenhan, W. P. Facsimile Programme. Report R-12805; U.K. Atomic Energy Research Establishment, Harwell, 1987.
- Slagle, I. R.; Gutman, D.; Davies, J. W.; Pilling, M. J. *J. Phys. Chem.* **1988**, *92*, 2455.
- Baulch, D. L.; Cobos, C. J.; Cox, R. A.; Esser, C.; Frank, P.; Just, Th.; Ken, J. A.; Pilling, M. J.; Troe, J.; Walker, R. W.; Warnatz, J. *J. Phys. Chem. Ref. Data* **1992**, *21*, 411.
- Nesbitt, F. L.; Marston, G.; Stief, L. *J. Phys. Chem.* **1990**, *94*, 4946.
- Baulch, D. L.; Duxbury, J.; Grant, S. J.; Montague, D. C. *J. Phys. Chem. Ref. Data, Suppl.* **1981**, *10*, 1.
- Seeger, C.; Rotzall, G.; Lulbert, A.; Schugerl, K. *Int. J. Chem. Kinet.* **1981**, *13*, 39.
- Tsang, W. Private communication.
- Lias, S. G.; Bartmess, J. E.; Liebman, J. F.; Holmes, J. L.; Levin, R. D.; Mallard, W. G. *J. Phys. Chem. Ref. Data, Suppl.* **1988**, *17*, 1.
- Foner, S. N.; Hudson, R. L. *J. Chem. Phys.* **1978**, *68*, 2987.
- Kiefer, J. H.; Mitchell, K. I.; Wei, H. C. *Int. J. Chem. Kinet.* **1988**, *20*, 787.
- Carr, R. W.; Walters, W. D. *J. Phys. Chem.* **1965**, *69*, 1073.
- Benson, S. W.; O'Neal, H. E. *Kinetic Data on Gas Phase Unimolecular Reactions*; National Standard Reference Data Series 21; National Bureau of Standards: Washington, DC, 1970.
- Woodward, R. B.; Hoffmann, R. *The Conservation of Orbital Symmetry*; Verlag Chemie Academic Press: Germany, 1970.
- Gilbert, R. G.; Smith, S. C. *Theory of Unimolecular and Recombination Reactions*; Blackwell Scientific Publications: London, 1990.
- Tardy, D. C.; Rabinovitch, B. S. *Chem. Rev.* **1977**, *77*, 369.
- Rabinovitch, B. S.; Diesen, R. W. *J. Chem. Phys.* **1959**, *30*, 735.
- Marcus, R. A. *J. Chem. Phys.* **1952**, *20*, 359.
- Oref, I. *J. Phys. Chem.* **1989**, *93*, 3463.
- Shimanouchi, T. *Tables of Molecular Vibrational Frequencies Part 3*; National Standard Reference Data Series 17; National Bureau of Standards, Washington, DC, 1968.
- Nielsen, I. M. B.; Janssen, C. L.; Burton, N. A.; Schaefer, H. F. *J. Phys. Chem.* **1992**, *96*, 2490.